Synthesis of Silver Nanoparticles using Non-Fouling Microfluidic Devices with Fast Mixing

Razwan BABER [1], Luca MAZZEI [1], Nguyen T. K. THANH [2,3], Asterios GAVRIILIDIS [1,*]

* Corresponding author: Tel.: +44 (0) 20 76793811; Email: a.gavriilidis@ucl.ac.uk
1 Department of Chemical Engineering, University College London, UK
2 UCL Healthcare Biomagnetic and Nanomaterials Laboratories
3 Department of Physics and Astronomy, University College London, UK

Abstract: Silver nanoparticles were synthesized in an impinging jet reactor using silver nitrate as a precursor, trisodium citrate as a stabilizer and sodium borohydride as a reducing agent. The effect of mixing time on the nanoparticle morphology was investigated by means of UV-Vis spectroscopy, used as a characterization tool. It was observed that as the mixing time became shorter the nanoparticles retained a similar average diameter but produced more aggregates. The mixing time was characterized using the 'Villermaux-Dushmann' reaction system together with the Interaction by Exchange with the Mean mixing model. The mixing time achieved was of the order of a few ms for flowrates in the range 18-28 ml/min. The synthesis of silver nanoparticles was carried out at the same flowrates to link mixing time to silver nanoparticle morphology.

Keywords: Micromixing, Impinging jet, Nanomaterials, Nanocrystallisation

1. Introduction

Nanoparticles (NPs) are materials which differ from their bulk counterparts because they exhibit unique properties. These properties arise from their relatively small size, leading to the potential for a vast amount of applications. In the case of nanosilver, applications include use in gas sensors (Bahadur et al., 2011; Korotcenkov et al., 2012), optics (Evanoff and Chumanov, 2005; Murphy et al., 2005; Panigrahi et al., 2006), electronics (Chen et al., 2009; Li et al., 2005), catalysis (Link et al., 1999; Patel et al., 2007) and biomedicine (Sharma et al., 2009; Sotiriou and Pratsinis, 2011).

The properties of the NPs depend on their size, composition and morphology, making them very different from their bulk counterparts which retain their properties irrespective of size. NPs exhibit a large surface area to volume ratio, which changes significantly with increasing size in the scale between 1 and 100 nm, resulting in changing properties of the NPs. The most obvious example of this change in properties with size is quantum dots which exhibit different colours on exposure to ultraviolet light depending on their size (Chan et al., 2002; Leutwyler et al., 1996).

When considering the "bottom-up" chemical synthesis approach to making NPs, most studies employ the use of reactors consisting of a vessel which is mechanically stirred. In chemical engineering terms, these reactions are carried out in a "batch" reactor. The benefits of using such reactors suit the aim of discovering new synthetic methods involving different concentrations, temperatures and reagents in a relatively simple manner. More recently, microfluidic devices have been employed to synthesise NPs because of the various benefits offered by these types of reactors (Zhao et al., 2011). These include improved heat and mass transfer, efficiency and safety (Gavriilidis et al., 2002). Due to these enhanced characteristics, improvements in the morphological characteristics of NPs synthesized by means of chemical methods can be made (i.e. narrow size distributions and control of size

In this study, an investigation on the effect of mixing on the repeatable synthesis and morphology of silver NPs is carried out.). An impinging jet reactor is used which avoids

fouling because the reagents do not come into contact with walls as in traditional microfluidic devices. The aim is to clarify the role of mixing in the synthesis of NPs and how this affects the resultant size and size distribution. The repeatability of the synthesis is of equal importance (to ensure reliable data) and hence it is also an aim to establish the suitability of any microfluidic device used by checking if it is able to produce repeatable results. Currently, many studies in the literature focus on the effects of changing various concentration parameters such as surfactant, precursor and reducing agent concentrations. Although these are very important parameters, mixing is intimately linked with concentration especially when the kinetics of the reaction are faster than the mixing kinetics. Although many studies attempt to elucidate the growth mechanisms involved in the synthesis of silver NPs, it is unclear without confirmation on the mixing and reaction kinetics whether these growth mechanisms are specifically applicable to the conditions used or whether they have a wider and more general applicability.

2. Methodology

2.1 Mixing characterization

The Villermaux-Dushman test reaction system (Guichardon and Falk, 2000) was employed as a means to characterise the mixing efficiency of the devices used. Sulfuric acid (H_2SO_4, 3 M stock solution, Alfa Aesar), potassium iodide (KI, 99%, Sigma), potassium iodate (KIO_3, 98%, Sigma) and boric acid (H_3BO_3, 99.5%, Sigma) were used.

This type of reaction system allows obtaining a mixing time for any micromixer by tuning the concentrations used in the reaction appropriately. The reactions are as follows:

$$H_2BO_3^- + H^+ \leftrightarrow H_3BO_3 \qquad (1)$$
$$5I^- + IO_3^- + 6H^+ \leftrightarrow 3I_2 + 3H_2O \qquad (2)$$
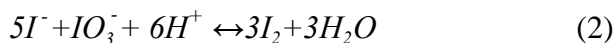
Reaction 1 is considered instantaneous and reaction 2 is considered fast. Sulphuric acid is

introduced to a mixture of borate, iodide and iodate ions. If mixing is very fast then only reaction 1 occurs. If mixing is slower, reaction 2 can occur. This is because if mixing is imperfect then all the orthoborate ions in the local region are consumed, leaving only iodide and iodate ions for the sulphuric acid to react with. Sulphuric acid is introduced in stoichiometric defect with respect to orthoborate ions to ensure that reaction 2 only proceeds if the orthoborate ions in the local region are consumed rather than because of an excessive amount of acid. The extent to which reaction 2 can take place gives an indication of the mixing efficiency. Iodine formed in reaction 2 further reacts with iodide to form triiodide:

$$I_2 + I^- \leftrightarrow I_3^- \qquad (3)$$

The concentration of triiodide ions formed gives the extent to which reaction 2 has occurred (and hence the mixing efficiency) and is measured using UV-Vis spectrometry. Triiodide exhibits a strong peak at 353 nm enabling its concentration to be calculated. The extinction coefficient of triiodide was found to be 25878 $M^{-1} \cdot cm^{-1}$ at 353 nm, found to be in good agreement with the literature (Guichardon and Falk, 2000). The micromixing quality is quantified by the segregation index:

$$X_S = \frac{Y}{Y_{ST}} \qquad (4)$$

Where:

$$Y = \frac{2([I_2] + [I_3^-])}{\alpha [H^+]_0}$$

$$Y_{ST} = \frac{6[IO_3^-]_0}{[H_2BO_3^-]_0 + 6[IO_3^-]_0}$$

where α is defined as the volumetric flowrate of acid over the volumetric flowrate of borate, iodide and iodate ions. When segregation index approaches zero, the mixing quality is perfect; conversely, when it approaches one,

perfect segregation is present.

The segregation index can be linked to the mixing efficiency through the use of a mixing model. The Interaction by Exchange with the Mean (IEM) model was used (Falk and Commenge, 2010).

2.2 Nanoparticle synthesis

Silver nanoparticles were synthesised by adding a mixture of silver nitrate ($AgNO_3$, 0.01 M stock solution, Sigma) and trisodium citrate ($HOC(COONa)(CH2COONa)_2 \cdot 2H_2O$, powder form, Sigma) to a sodium borohydride solution ($NaBH_4$, ~12 wt% in 14 M NaOH stock solution, Sigma). All chemicals were used without further purification and solutions were prepared with ultrapure water (resistivity 15.0 MΩ·cm). Syringe pumps (Cavro XP3000, Tecan) were used to deliver the two inputs of a mixture of silver nitrate/trisodium citrate solution and a sodium borohydride solution to an impinging jet reactor (IJR). Two devices were employed, IJR-1 and IJR-2. Mixing efficiency was varied by altering the total flowrate of the input streams while keeping the flow ratio between the two streams constant at 1:1. The silver NPs were analysed using a UV-Vis spectrophotometer (UV-2550, Shimadzu). The particles were pipetted into a 1 cm x 1 cm plastic cuvette without any further treatment before being placed in the spectrometer.

3. Results and discussion

3.1 Mixing characterization

To relate mixing time to the segregation index, the IEM mixing model must be solved. The gProms model builder software (gProms version 3.20) was used to solve the set of ordinary differential mass balance equations over an appropriate range of mixing times. Fig. 1 shows the mixing time vs. segregation index curve obtained for the concentration set: 0.006 M potassium iodate, 0.032 M potassium iodide, 0.045 M sodium hydroxide, 0.09 M orthoboric acid and 0.017 M sulphuric acid.

Experiments were carried out in the IJR-1 with the same concentration set used to obtain the mixing time vs. segregation index curve shown in Fig. 1. The triiodide concentration is measured using UV-Vis spectroscopy and then the segregation index is calculated. The mixing time can then be obtained from Fig.1. Fig. 2 shows mixing time vs. flowrate for 18-28 ml/min total flowrate, giving a mixing time in the range of 1-4 ms for IJR-1. This enables the mixing time to be linked to the silver NP synthesis.
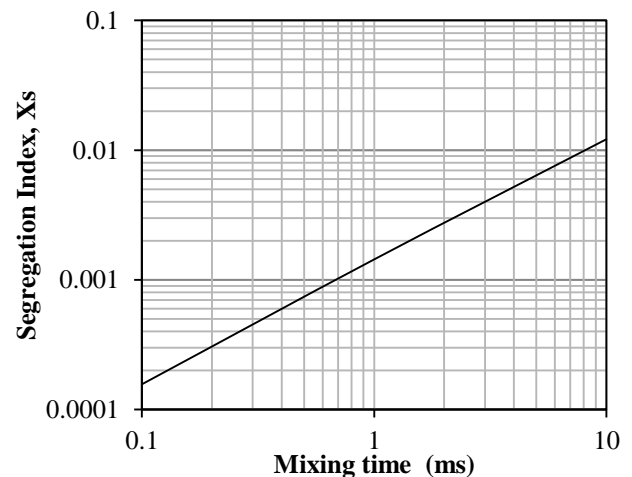
Fig. 1. Mixing time vs. segregation index for the concentration set: 0.006 M potassium iodate, 0.032 M potassium iodide, 0.045 M sodium hydroxide, 0.09 M orthoboric acid and 0.017 M sulphuric acid
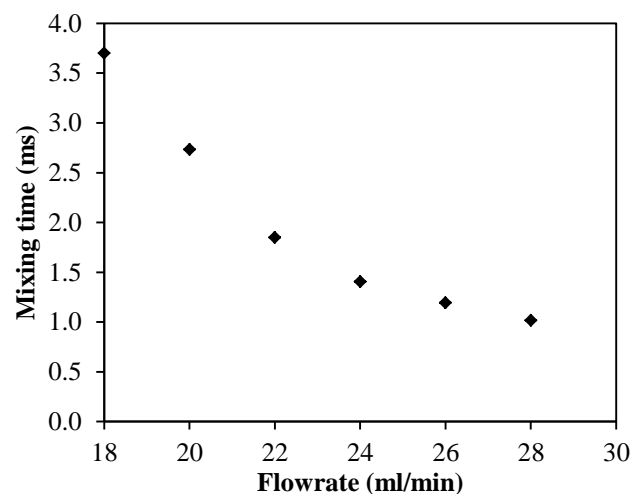
Fig. 2. Mixing time vs. total flowrate in IJR-1.

3.2 *Nanoparticle synthesis*

The repeatability of the silver NP synthesis was tested for IJR-2. The synthesis was performed five times and the deviation in peak absorbance and full width at half maximum (FWHM) of the UV-Vis spectra is used as an indicator of synthesis repeatability. Fig. 3 shows the UV-Vis spectra of the 5 experiments. The peak absorbance relates to the concentration of the NPs, while the FWHM relates to the polydispersity of the NPs. The average peak absorbance of the synthesis is 0.49 with a deviation of 0.86% and the average FWHM is 95.8 nm with a deviation of 0.87%. This represents small amounts of variation in the synthesis indicating that the system is capable of repeatable results.
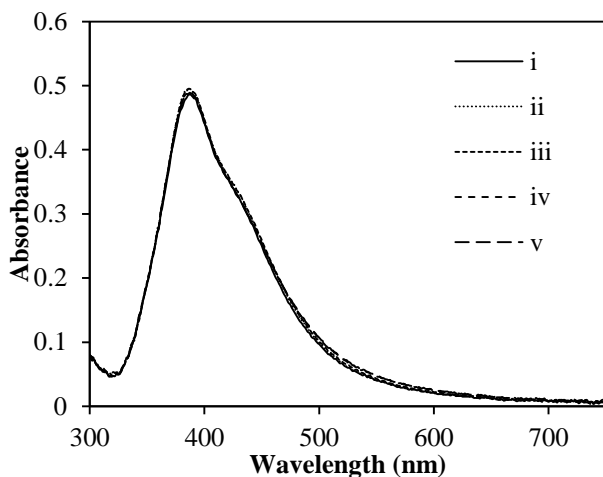

Fig. 3. UV-Vis spectra of silver NP syntheses (5 repeated experiments) using IJR-2. Final concentrations of reagents were 0.05 mM silver nitrate, 0.5 mM trisodium citrate and 0.15 mM sodium borohydride (0.482 mM NaOH)

Following the repeatability experiments, the effect of mixing efficiency was investigated in IJR-1. The total flowrate was varied to change the mixing efficiency between experiments while keeping the final concentrations and inlet flow ratio (1:1) constant. Fig. 4 shows the UV-Vis spectra for samples obtained at various flowrates between 18 ml/min and 28 ml/min.

Fig. 5 shows the peak absorbance and FWHM plotted as a function of mixing time for the spectra shown in Fig. 4. Fig. 6 shows that as mixing time decreases, peak absorbance decreases and FWHM increases. Fig. 6 shows mixing time vs. peak wavelength (the peak wavelength represents the average size of the particles) for the syntheses. The wavelength does not change significantly with mixing time. Two observations can be made from the results. Firstly, the concentration of silver NPs decreases (because the absorbance drops) and the particle size distribution becomes more polydisperse (because the FWHM increases) as the mixing time decreases (faster mixing). Shoulders appear in the spectra as mixing becomes faster (a shoulder in the peak absorbance indicates the presence of larger particles which are possibly aggregates); Hence, it is possible that as the flowrate increases, the amount of aggregates or large particles in the final solution increases (also possibly a combination of large particles and aggregates).
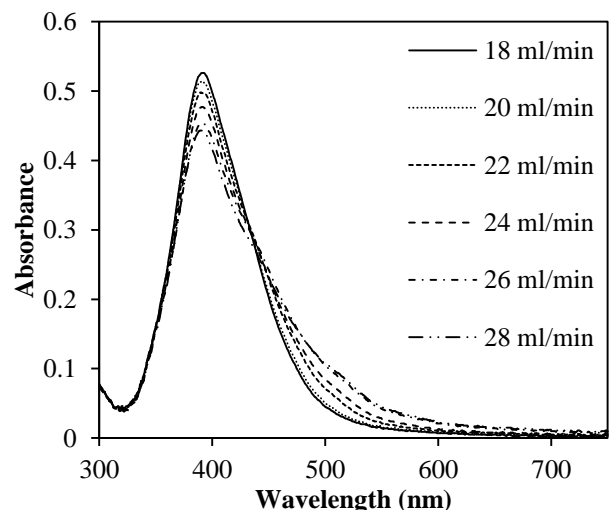

Fig. 4. UV-Vis spectra of silver NP syntheses performed at various flowrates with IJR-1. Final concentrations of reagents were 0.45 mM silver nitrate, 3 mM trisodium citrate, 0.9 mM sodium borohydride and 2.89 mM NaOH. A 1:1 flow ratio was used in all cases. The samples were diluted by a factor of 10.

Secondly, the predominant (in terms of number) size of the particles in the solution does not change significantly. At higher flowrates (shorter mixing time) the IJR

produces a lower concentration of NPs because there are fewer smaller particles and a higher amount of larger particles (although the predominant size of the particles does not change significantly).

The results are the opposite of the expected outcome which was that a faster mixing time would result in NPs with lower polydispersity, because that by increasing mixing efficiency, the reactants approach a homogeneous concentration profile quicker. If there are differences in local concentrations, it is expected that different levels of saturation and supersaturation will occur. This would result in different nucleation and growth rates, resulting in a more polydisperse final NP solution. However, the reduction reactions for the formation of NPs are known to be quick and the mixing may still not be efficient enough to be faster than the reaction rate. By achieving faster mixing, the effect of an evolving concentration profile is expected to be reduced as the reaction proceeds. It is unclear at this stage why there is an increase in polydispersity as the mixing time decreases but it is likely to be related to a concentration/hydrodynamic effect (i.e. the evolution of concentrations as mixing and reaction proceeds).
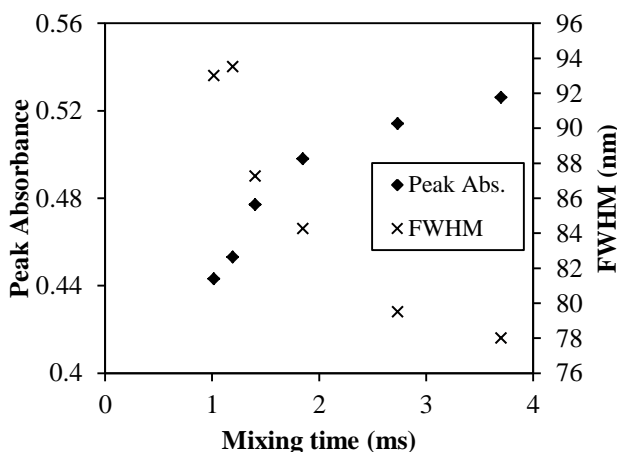

Fig. 5. Mixing time vs. peak absorbance (left axis) and mixing time vs. FWHM (right axis) for the silver NP synthesis from 18 ml/min (3.7 ms) and 28 ml/min (1 ms). Fig.4 shows the UV-Vis spectra for the synthesis.
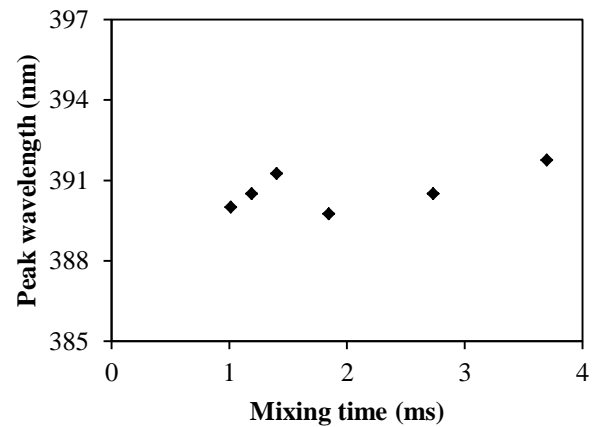

Fig. 6. Mixing time vs. peak absorbance location for the silver NP synthesis from 18 ml/min (3.7 ms) and 28 ml/min (1 ms). Fig. 4 shows the UV-Vis spectra for the synthesis

4. Conclusions

For the system and conditions studied, as the mixing time becomes faster the silver NPs appear to produce more aggregates but retain a similar predominant size. The IJR is capable of highly repeatable silver NP synthesis and mixing times between 1-4 ms were achieved. This is still larger than the characteristic reaction time for the reduction of silver ions to silver metal preceding nucleation and growth steps in the reaction. To obtain truly separated and defined nucleation and growth periods, the mixing kinetics must be faster than the reaction kinetics.

5. References

Bahadur, N., Jain, K., Pasricha, R., Govind, Chand, S., 2011. Selective gas sensing response from different loading of Ag in sol–gel mesoporous titania powders. Sensors and Actuators B: Chemical 159, 112-120.

Chan, W.C., Maxwell, D.J., Gao, X., Bailey, R.E., Han, M., Nie, S., 2002. Luminescent quantum dots for multiplexed biological detection and imaging. Current opinion in biotechnology 13, 40-46.

Chen, D., Qiao, X., Qiu, X., Chen, J., 2009. Synthesis and electrical properties of

uniform silver nanoparticles for electronic applications. J Mater Sci 44, 1076-1081.

Evanoff, D.D., Chumanov, G., 2005. Synthesis and Optical Properties of Silver Nanoparticles and Arrays. ChemPhysChem 6, 1221-1231.

Falk, L., Commenge, J.M., 2010. Performance comparison of micromixers. Chem Eng Sci 65, 405-411.

Gavriilidis, A., Angeli, P., Cao, E., Yeong, K.K., Wan, Y.S.S., 2002. Technology and applications of microengineered reactors. Chemical Engineering Research & Design 80, 3-30.

Guichardon, P., Falk, L., 2000. Characterisation of micromixing efficiency by the iodide-iodate reaction system. Part I: experimental procedure. Chem Eng Sci 55, 4233-4243.

Korotcenkov, G., Cho, B.K., Gulina, L.B., Tolstoy, V.P., 2012. Gas sensor application of Ag nanoclusters synthesized by SILD method. Sensors and Actuators B: Chemical 166–167, 402-410.

Leutwyler, W.K., Bürgi, S.L., Burgl, H., 1996. Semiconductor clusters, nanocrystals, and quantum dots. Science 271, 933.

Li, Y., Wu, Y., Ong, B.S., 2005. Facile synthesis of silver nanoparticles useful for fabrication of high-conductivity elements for printed electronics. J Am Chem Soc 127, 3266-3267.

Link, S., Wang, Z.L., El-Sayed, M., 1999. Alloy formation of gold-silver nanoparticles and the dependence of the plasmon absorption on their composition. The Journal of Physical Chemistry B 103, 3529-3533.

Murphy, C.J., Sau, T.K., Gole, A.M., Orendorff, C.J., Gao, J., Gou, L., Hunyadi, S.E., Li, T., 2005. Anisotropic metal nanoparticles: synthesis, assembly, and optical applications. The Journal of Physical Chemistry B 109, 13857-13870.

Panigrahi, S., Praharaj, S., Basu, S., Ghosh, S.K., Jana, S., Pande, S., Vo-Dinh, T., Jiang, H., Pal, T., 2006. Self-assembly of silver nanoparticles: Synthesis, stabilization, optical properties, and application in surface-enhanced Raman scattering. Journal of Physical Chemistry B 110, 13436-13444.

Patel, A.C., Li, S., Wang, C., Zhang, W., Wei, Y., 2007. Electrospinning of porous silica nanofibers containing silver nanoparticles for catalytic applications. Chemistry of materials 19, 1231-1238.

Sharma, V.K., Yngard, R.A., Lin, Y., 2009. Silver nanoparticles: Green synthesis and their antimicrobial activities. Advances in Colloid and Interface Science 145, 83-96.

Sotiriou, G.A., Pratsinis, S.E., 2011. Engineering nanosilver as an antibacterial, biosensor and bioimaging material. Current Opinion in Chemical Engineering 1, 3-10.

Zhao, C.-X., He, L., Qiao, S.Z., Middelberg, A.P.J., 2011. Nanoparticle synthesis in microreactors. Chem Eng Sci 66, 1463-1479.